

Supporting Information

Interfacial Reactions of Cu(II) Adsorption and Hydrolysis Driven by Nano-scale Confinement

Andrew W. Knight¹, Poorandokht Ilani-Kashkouli², Jacob A. Harvey³, Jeffery A. Greathouse³, Tuan A. Ho³, Nadine Kabengi^{2,4}, and Anastasia G. Ilgen^{3*}

¹Storage and Transport Technologies Department, Sandia National Laboratories, Albuquerque, NM 87185-0754, United States

²Department of Geosciences, Georgia State University, Atlanta, Georgia 30303.

³Geochemistry Department, Sandia National Laboratories, Albuquerque, NM 87185-0754, United States

⁴Department of Chemistry, Georgia State University, Atlanta, Georgia 30303

Samples for XAFS

The amount of Cu²⁺ adsorbed on each silica material was quantified by ICP-MS and normalized by surface area. For each material, a low (lCu), medium (mCu), and high (hCu) surface loading were prepared, however only the fumed silica-hCu, SBA-15-4-mCu, SBA-15-4-hCu, SBA-15-8-mCu, and SBA-15-8-hCu were analyzed by XAFS.

Due to the close proximity of Cu-Si and Cu-Cu backscattering features in XAFS spectra, and the backscattering signal from the Cu-Si shell being weaker, Cu-Si becomes nearly invisible with increasing proportion of polynuclear copper species on the surface. We fit all data including and excluding the Cu-Si shell, and a statistically significant improvement of the fit was only seen for the SBA-15-4-hCu sample (Table S1).

Table S1. Summary of XAFS fits with and without including Cu-Si shell.

Material	r-range	XAFS Fit	R-factor	Reduced χ^2	Independent Points
Fumed silica-hCu	1.0-5.0	With Cu-Si Shell	0.020	31.40	22.05
		Without Cu-Si Shell	0.020	32.74	22.05
SBA-15-8-hCu	1.0-5.0	With Cu-Si Shell	0.026	48.07	22.02
		Without Cu-Si Shell	0.026	50.40	22.05
SBA-15-8-mCu	1.0-5.0	With Cu-Si Shell	0.021	28.60	22.05
		Without Cu-Si Shell	0.021	27.28	22.05
SBA-15-4-hCu	1.0-5.0	With Cu-Si Shell	0.009	34.14	22.04
		Without Cu-Si Shell	0.015	82.38	22.04
SBA-15-4-mCu	1.0-5.0	With Cu-Si Shell	0.024	59.04	22.05
		Without Cu-Si Shell	0.028	67.40	22.05

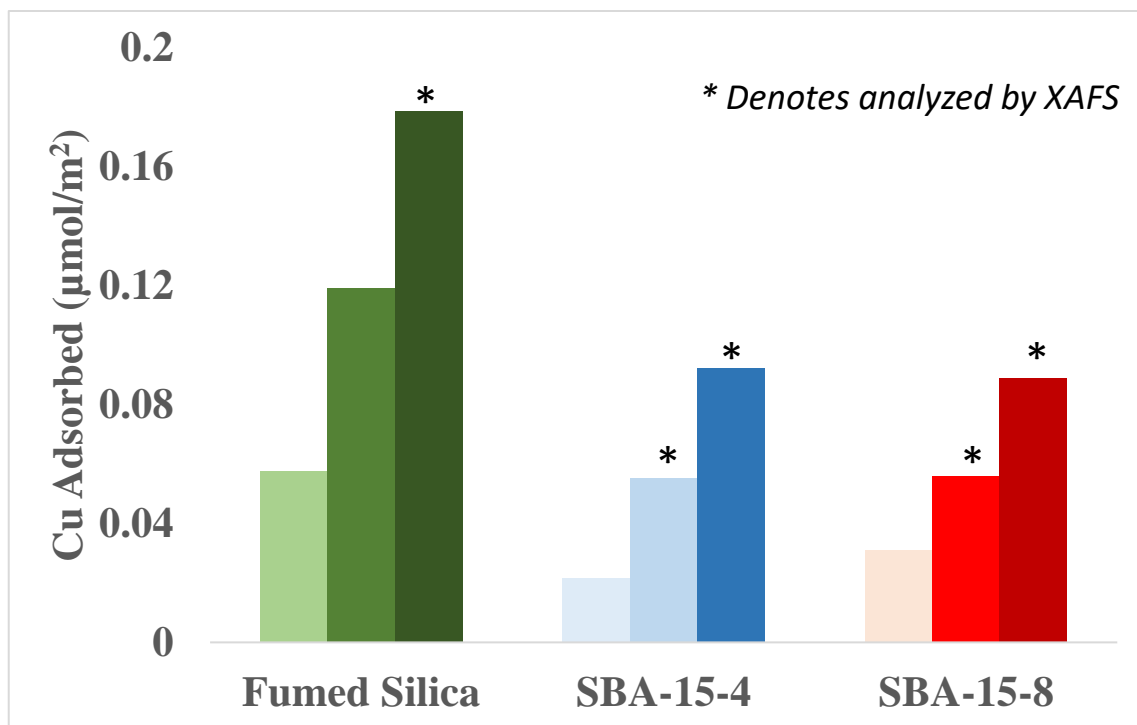


Figure S1. Surface loading for high, medium, and low Cu adsorption on silica materials. The asterisk denotes samples that were analyzed by XAFS.

Calorimetry

Chemical and physical parameters of the species involved in the calorimetric studies are shown in **Table S2**.

Table S2. Hydration enthalpies, ionic radii, hydration radii, and hydration numbers for ionic species used in calorimetric analyses.

Ion	Hydration Enthalpies (kJ/mol)	Ionic Radii (Å)	Hydration Radii (Å)	Hydration Numbers
Cu ²⁺	593	0.96	4.19	4, 5, and 6
Na ⁺	409	1.02	3.58	6
NH ₄ ⁺	307	1.48	3.39	4–8

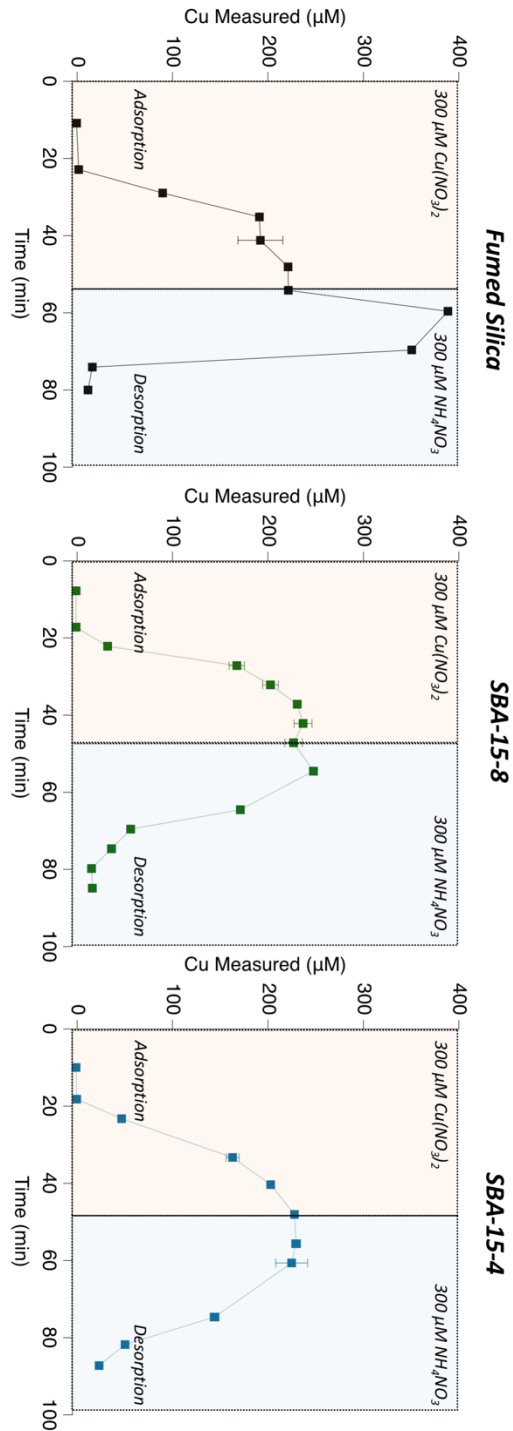


Figure S2. Adsorption and desorption of Cu on fumed silica, SBA-15-8, and SBA-15-4 from flow through calorimetric studies, quantified by ICP-MS. The adsorption branch consisted of adding 300 µM Cu(NO₃)₂ at a rate of 0.3 mL/min, and the desorption branch consisted of adding 300 µM NH₄NO₃ at 0.3 mL/min.

Molecular Modeling

Silica Nano-scale Pore Models

To generate the amorphous silica surface model, a $12 \times 12 \times 6$ supercell (8640 atoms) was created from the β -cristobalite unit cell. The supercell was then heated from 298 K to 4000 K over a 1 ns simulation during which the temperature and pressure were controlled using the Berendsen thermostat and barostat.¹ A constant 1 atm pressure was maintained with a 1000 fs damping parameter and a 3.6×10^4 atm bulk modulus, while the temperature was maintained with a 100 fs damping parameter. The pressure in the x and y directions were coupled while the z direction fluctuated independently in order to produce a square slab. Upon reaching a temperature of 4000 K, an additional 1 ns simulation was performed at this temperature to ensure equilibrium and that a properly melted structure resulted. The melted silica slab was contained in a $65.674 \times 65.674 \times 38.154$ Å box. A 5 nm vacuum layer was then added to both sides of the surface (10 nm total) and the slab was cooled from 4000 to 300 K over 37 ns for a cooling rate of $0.1 \text{ K}\cdot\text{ps}^{-1}$. The final structure was equilibrated for an additional 0.25 ns at 300 K. Cooling was performed in the *NVT* ensemble (number of particles, volume, temperature), where the temperature was controlled with the Berendsen thermostat and the same parameters previously mentioned. This method of cooling with a vacuum layer results in non-atomically flat interface with the interface existing in the xy plane. The calculated total surface area (both sides) of the silica slab was 138.38 nm^2 , compared to the xy surface area of 42.13 nm^2 , indicating that significant roughening had occurred.

Functionalizing the surface with hydroxyl groups occurred in two steps. First, the coordination shell of all silicons and oxygens were augmented to 4 and 2, respectively, by adding OH and H groups. However, in order to maintain charge neutrality, identical numbers of OH and H groups have to be added. Note that only atoms with a local density of less than $1.4 \text{ g}\cdot\text{cm}^{-3}$ were allowed to be functionalized, which represents 66% of the maximum density ($2.1 \text{ g}\cdot\text{cm}^{-3}$, **Fig. S3**). Site densities were calculated within an 8 Å radius. The consequence of this density-driven approach is that sites in the interior of the slab can also be functionalized. A different approach would be to define an arbitrary z value, or distance from slab center, and limit functionalization to outside of that region. However, it is challenging to choose an appropriate value given a non-atomically flat surface. During this step of functionalization both singly and doubly functionalized (silanol/geminol) Si atoms formed. This procedure led to 148 silanols and 42 geminols for an OH site density of $1.68 \text{ OH}\cdot\text{nm}^{-2}$.

In order to increase the OH density, “long” Si-O bonds were broken, and water added across the bond to produce two new hydroxyls. The definition of a “long” bond was chosen arbitrarily such that the target OH density of $\sim 2.0 \text{ OH}\cdot\text{nm}^{-2}$ was reached on both sides of the surface. Additionally, the density criteria listed above was applied, and the O atom had to be more exposed than either neighboring Si atom. New hydroxyls were added perpendicular to the surface and overlapping hydroxyls were slightly rotated to avoid high repulsive forces. The final surface consisted of 174 silanols, 48 geminols, 2658 slab Si’s, and 5625 slab O’s for a final OH site density of $1.95 \text{ OH}\cdot\text{nm}^{-2}$. This process ensured that the resulting silica surfaces have significant roughness (nonplanar), yet they are fully flexible and remain stable during the simulations.

Negative surface charge corresponding to experimental pH conditions ($-0.25 \text{ C}\cdot\text{m}^{-2}$) was obtained by removing 17 H atoms on each side of the slab. Silanol-only hydroxyl groups were chosen at random producing a visually heterogenous surface, resulting in a loss of $0.425 e$ per site, where e is the elementary charge. The remaining $-0.575 e$ was distributed on the Si and O atoms, resulting in a net charge of $-1.0 e$ per siloxide (SiO^-) site. Smearing the excess charge over a larger area of the surface did not have a significant effect on the adsorption properties and this localized approach provides the simplest method of implementation.

To generate aqueous nanopore models, the z -dimension of the dry silica nanopore model was expanded and 17 Cu^{2+} ions were randomly inserted into the vacuum region to balance the surface charge. An additional number of Cu^{2+} and OH^- ions were inserted, corresponding to a Cu^{2+} concentration of approximately 0.1 M at each pore diameter (2, 4, and 8 nm). To investigate the dependence on initial Cu

coordination environment, separate nanopore models were created in which $[\text{Cu}_2(\text{OH})_2]^{2+}$ dimers were initially inserted using all available OH^- ions. Changes in the adsorption process (**Fig. S4**) as well as calculated radial distribution functions (RDFs, **Table S3**) for simulations started as Cu dimers or Cu monomers were minimal, therefore all results depicted in the main manuscript were generated from the monomer start simulations. Finally, an appropriate number of water molecules were inserted to achieve the desired pore diameter after equilibration. The filled porous structures were then minimized under constant volume conditions. After minimization, the water molecules only were simulated in the *NVT* ensemble using the Nose-Hoover thermostat at 500 K for 0.2 ns, followed by a simulation in which water and ions were heated from 500 K to 1000 K over 0.2 ns, followed by an additional 0.2 ns at 1000 K to ensure proper mixing, then cooled to 300 K over 0.2 ns, and then finally equilibrated at 300 K for an additional 0.2 ns. The entire system (surface included) was then equilibrated first in the *NPT* ensemble (number of particles, pressure, temperature) for 1 ns to allow the pore size to relax, and then in the *NVT* ensemble for 10.0 ns. The fluid composition and equilibrated pore diameter of each model system is given in **Table S4**.

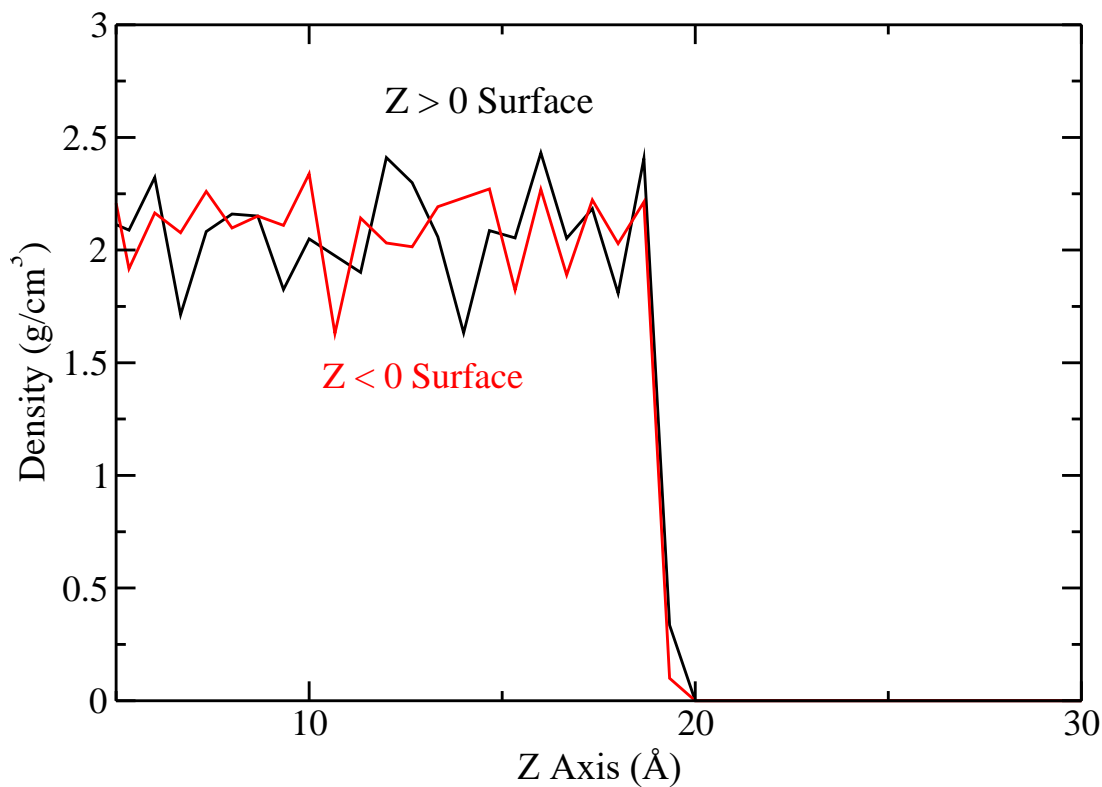


Figure S3. Density of the silica surface as a function of position along the axis perpendicular to the surface for the upper (black) and lower (red) sides.

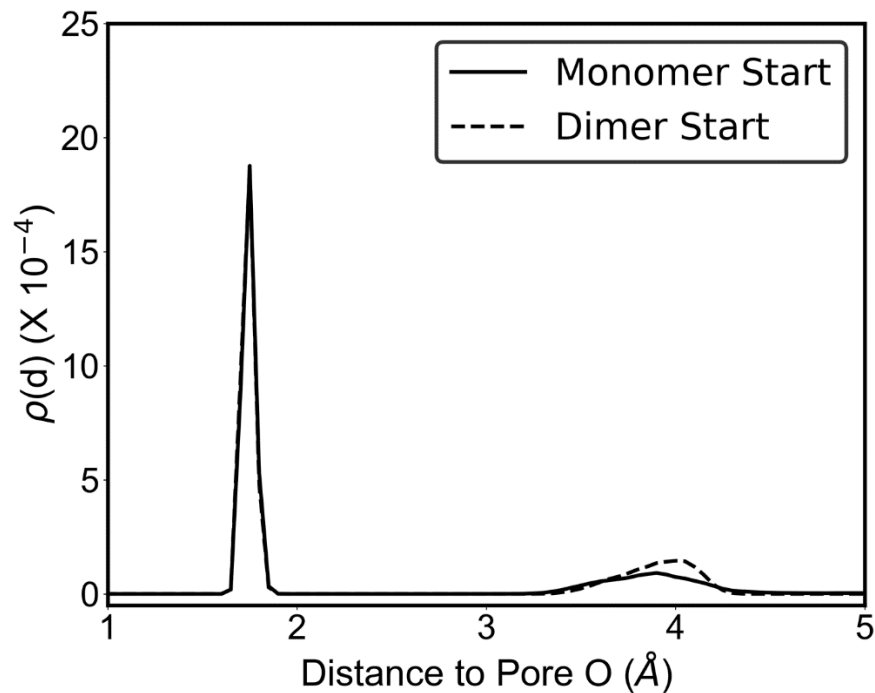


Figure S4. Cu number density as a function of distance to the nearest pore O for simulations where Cu was inserted as a dimer (dashed) or monomer (solid).

Table S3. Cu average distance and coordination number determined from simulated RDFs. Shown are values for Cu- deprotonated oxygens, hydroxyl ion oxygens, water oxygens, as well as Cu-Cu and Cu-Si. Results for the monomer start from the main manuscript are repeated here to compare alongside the dimer start simulations.

Sample	Shell	Start with Monomers		Start with Dimers	
		CN	R (Å)	CN	R (Å)
8 nm Pore	Cu-O _{dep}	0.42	1.75	0.39	1.75
	Cu-O	1.88	1.78	2.19	1.79
	Cu-O _w	2.74	1.98	2.41	1.98
	Cu-Cu	0.59	2.65	0.89	2.62
	Cu-Si	0.41	3.15	0.39	3.08
4 nm Pore	Cu-O _{dep}	0.58	1.75	0.52	1.75
	Cu-O	1.17	1.75	1.74	1.80
	Cu-O _w	3.36	1.98	2.94	2.01
	Cu-Cu	0.26	2.68	0.71	2.65
	Cu-Si	0.58	3.15	0.52	3.15
2 nm Pore	Cu-O _{dep}	0.69	1.78	0.69	1.75
	Cu-O	1.05	1.78	1.38	1.80
	Cu-O _w	3.58	1.98	3.26	2.02
	Cu-Cu	0.35	2.65	0.69	2.62
	Cu-Si	0.69	3.12	0.69	3.15

Table S4. Fluid Composition and Diameter of Nanopore Models

Cu ²⁺	OH ⁻	H ₂ O	diameter (nm) ^a
26	18	4368	2.78
31	28	7280	4.72
41	48	12640	8.39

^a Obtained using the HOLE code ² after equilibration at 300 K. Taken as an average at several points within the pore.

Interaction Parameters for MD simulations

LAMMPS format with units "real"

Masses

1 28.0855
2 15.9994
3 1.0079
4 28.0855
5 15.9994
6 15.9994
7 15.9994
8 1.00797
9 63.55
10 15.9994
11 1.00797

Pair Coeffs # lj/cut/coul/long

1	1.8402e-06	3.30196	# st
2	0.155416	3.16552	# oh
3	0		# ho
4	1.8402e-06	3.30196	# sdep (Si at SiO ⁻ site)
5	0.155416	3.16552	# odep (O at SiO ⁻ site)
6	0.155416	3.16552	# ob
7	0.15539	3.1656	# o* (SPC water)
8	0		# h* (SPC water)
9	0.0427	1.8406	# Cu ²⁺
10	0.15539	3.1656	# OH (hydroxide O)
11	0		# HO (hydroxide H)

Bond Coeffs # harmonic

1	553.935	1	# OH-HO and o*-h*
---	---------	---	-------------------

Angle Coeffs # harmonic

1	15	100	# st-oh-ho
2	45.77	109.47	# h*-o*-h*

Atom Charges

1 2.100
2 -0.950
3 0.425
4 1.960
5 -1.385
6 -1.050
7 -0.820
8 0.410
9 2.000
10 -1.410
11 0.410

1. H. J. C. Berendsen, J. P. M. Postma, W. F. van Gunsteren, A. DiNola and J. R. Haak, Molecular dynamics with coupling to an external bath, *J. Chem. Phys.*, 1984, **81**, 3684-3690.

2. O. S. Smart, J. G. Neduelil, X. Wang, B. A. Wallace and M. S. P. Sansom, HOLE: A program for the analysis of the pore dimensions of ion channel structural models, *J. Mol. Graphics Modell.*, 1996, **14**, 354-360.